The Plant Cell, Vol. 31: 1222–1237, June 2019, www.plantcell.org © 2019 ASPB.

Genetic Interactions and Molecular Evolution of the Duplicated Genes *ICARUS2* and *ICARUS1* Help Arabidopsis Plants Adapt to Different Ambient Temperatures

Belén Méndez-Vigo,[a,1] Israel Ausín,[a,1] Wangsheng Zhu,[b,2] Almudena Mollá-Morales,[a] Sureshkumar Balasubramanian,[b] and Carlos Alonso-Blanco[a,3]

[a] Centro Nacional de Biotecnología, Consejo Superior de Investigaciones Científicas, 28049, Madrid, Spain
[b] School of Biological Sciences, Monash University, Victoria 3800, Australia

ORCID IDs: 0000-0002-9850-53 (B.M.-V.); 0000-0002-3707-1780 (I.A.); 0000-0001-7773-3438 (W.Z.); 0000-0001-9465-0490 (A.M.-M.); 0000-0002-1057-2606 (S.B.); 0000-0002-4738-5556 (C.A.-B.)

Understanding how plants adapt to ambient temperatures has become a major challenge prompted by global climate change. This has led to the identification of several genes regulating the thermal plasticity of plant growth and flowering time. However, the mechanisms accounting for the natural variation and evolution of such developmental plasticity remain mostly unknown. In this study, we determined that natural variation at *ICARUS2* (*ICA2*), which interacts genetically with its homolog *ICA1*, alters growth and flowering time plasticity in relation to temperature in Arabidopsis (*Arabidopsis thaliana*). Transgenic analyses demonstrated multiple functional effects for *ICA2* and supported the notion that structural polymorphisms in *ICA2* likely underlie its natural variation. Two major *ICA2* haplogroups carrying distinct functionally active alleles showed high frequency, strong geographic structure, and significant associations with climatic variables related to annual and daily fluctuations in temperature. Genome analyses across the plant phylogeny indicated that the prevalent plant *ICA* genes encoding two $tRNA^{His}$ guanylyl transferase 1 units evolved ~120 million years ago during the early divergence of mono- and dicotyledonous clades. In addition, *ICA1*/*ICA2* duplication occurred specifically in the Camelineae tribe (Brassicaceae). Thus, *ICA2* appears to be ubiquitous across plant evolution and likely contributes to climate adaptation through modifications of thermal developmental plasticity in Arabidopsis.

INTRODUCTION

Plants must adapt their development and physiology to environmental cues that change across geography and time. In the past few years, climatic factors such as temperature have become a major focus, and large efforts are currently devoted to understanding the mechanisms involved in plant adaptation to ambient temperature (Bita and Gerats, 2013). In particular, annual plants are characterized by their developmental plasticity in relation to temperature, which is presumed to reflect adaptations to seasonal fluctuations (Nicotra et al., 2010). High, but not stressful, temperatures influence overall plant growth during the vegetative phase, producing a set of morphological changes that are referred to as thermomorphogenesis. These changes resemble the plant responses to shade avoidance and include long hypocotyls and petioles, as well as upward leaf bending (hyponasty; McClung et al., 2016; Quint et al., 2016). Genetic and molecular studies, mostly in the model plant Arabidopsis (*Arabidopsis thaliana*), are elucidating the mechanisms underlying such temperature-mediated responses. Recently, *PHYTOCHROME B* has been proposed to function as a thermosensor through its temperature-dependent reversion from the active to the inactive form (Jung et al., 2016; Legris et al., 2016). In addition, the transcription factor PHYTOCHROME INTERACTING FACTOR4 (PIF4) has been shown to play a central role in controlling thermomorphogenesis (Quint et al., 2016). *PIF4* is transcriptionally and posttranslationally regulated to integrate signals from light, the circadian clock, and several phytohormones such as gibberellins and brassinosteroids. PIF4 subsequently regulates auxin biosynthesis and signaling genes. Moreover, histone modifications and chromatin remodelling also contribute to thermomorphogenesis, as the dynamics of H2A.Z nucleosomes and histone deacetylation appear to be associated with the thermoregulation of gene expression (Quint et al., 2016; Tasset et al., 2018). On the other hand, ambient temperature also affects the major developmental transitions in the plant life cycle, such as flowering initiation, which is often, but not always, advanced by high temperature (Verhage et al., 2014; Méndez-Vigo et al., 2016). The thermoregulation of flowering time involves different molecular mechanisms, including the temperature-dependent splicing and nonsense-mediated mRNA decay of *FLOWERING LOCUS M* (*FLM*) and the temperature-induced degradation of *SHORT VEGETATIVE PHASE* (*SVP*; Lee et al., 2013; Sureshkumar et al., 2016); the regulation of the florigen-encoding genes *FLOWERING LOCUS T* (*FT*) and *TWIN SISTER OF FLOWERING LOCUS T* (*TSF*) by PIF4 and *SVP* (Kumar et al., 2012; Fernández et al., 2016); and a potential role for the regulation of microRNAs miR156 and

[1] These authors contributed equally to this work.
[2] Current address: Department of Molecular Biology, Max-Planck Institute for Developmental Biology, D-72076, Tübingen, Germany.
[3] Address correspondence to calonso@cnb.csic.es.
The author responsible for distribution of materials integral to the findings presented in this article in accordance with the policy described in the Instructions for Authors (www.plantcell.org) is: Carlos Alonso-Blanco (calonso@cnb.csic.es).
www.plantcell.org/cgi/doi/10.1105/tpc.18.00938

IN A NUTSHELL

Background: Plants adapt to seasonal and yearly fluctuations in ambient temperature by altering multiple aspects of their development, such as growth and the time to initiate flowering. These modifications in plant development depending on temperature are known as thermal developmental plasticity. In plants with a broad geographic distribution, individuals or varieties from different world regions have different types of plasticity, which reflect adaptations to different natural environments. Currently, few genes and molecular mechanisms involved in the adaptation of plants to different ambient temperatures are known.

Question: We wanted to find out how plants from different world regions adapt to different climate temperatures.

Findings: We identified two homologous genes, *ICARUS1* (*ICA1*) and *ICA2*, which are responsible for the differences in thermal developmental plasticity shown by natural varieties of the model plant Arabidopsis. Both genes interact genetically to affect plant traits such as growth and flowering time, as well as cellular features such as the number of copies of the genome, i.e., ploidy level. We found that Arabidopsis plants from different world locations harbor different natural mutations in *ICA2*, suggesting that this gene might be involved in plant adaptation to different climates. Finally, we discovered that very few of copies (mostly one or two) of *ICA* genes are present in all plants across evolution.

Next steps: We plan to explore the precise molecular function of *ICA* genes in plants and how this function is regulated by fluctuating temperatures.

miR172 by the *SQUAMOSA PROMOTER BINDING-LIKE* (*SPL*) gene family (Verhage et al., 2014).

In addition to environmental acclimation to high ambient temperature via developmental plasticity, plant evolutionary adaptation to climate involves genetic modifications of such phenotypic responses among natural populations (Franks et al., 2014). Arabidopsis studies have already identified several genes contributing to the natural variation in thermomorphogenic growth, such as the circadian clock gene *EARLY FLOWERING3* (*ELF3*; Box et al., 2015; Raschke et al., 2015) and likely *PIF4*, a gene downregulated by *ELF3* (Brock et al., 2010). Furthermore, natural variants of *FLM*, *FLOWERING LOCUS C* (*FLC*), and *FRIGIDA* affect the plasticity of flowering time in relation to high ambient temperature (Balasubramanian et al., 2006; Lutz et al., 2015, 2017; Méndez-Vigo et al., 2016; Sanchez-Bermejo and Balasubramanian, 2016). Structural and regulatory mutations in these genes have been shown to alter temperature-mediated plasticity. In particular, a missense mutation in *ELF3* and multiple deletions and insertions in the promoter or intron regions of the other genes have been reported as functional polymorphisms (Lutz et al., 2015; Raschke et al., 2015; Méndez-Vigo et al., 2016). In addition, natural variation at the *ICARUS1* (*ICA1*) gene has been shown to produce a very severe growth defect characterized by short hypocotyls, small leaf size, late flowering, and low fertility, specifically at elevated temperature (>27°C), but not at 21°C (Zhu et al., 2015). Two natural loss-of-function mutations have been found in Arabidopsis accessions Don-0 and Sij-4 that behave similarly to null mutant alleles in the Columbia (Col) background. Plants carrying such natural or artificial *ica1* loss-of-function mutations also display larger cells, blockage of the G2/M transition of the cell cycle, and increased endoreduplication at high temperature, as well as enhanced sensitivity to DNA damage (Zhu et al., 2015). Thus, *ICA1* is an essential gene required for growth at high temperature that affects the plastic responses mediated by ambient temperature and other fundamental processes.

ICA1 is the homolog of *Thg1* from humans and yeasts. *Thg1* encodes a $tRNA^{His}$ guanylyl transferase, an enzyme that regulates $tRNA^{His}$ maturation by catalyzing the addition of a G nucleotide specifically to the 5′ end of $tRNA^{His}$ (Gu et al., 2003; Heinemann et al., 2012). This gene is universal across all life kingdoms, from archaea to animals and plants, and the enzymatic activity of Thg1 has been extensively studied because, contrary to other nucleic acid polymerases, it synthesizes 3′-to-5′ RNA (Heinemann et al., 2012; Lee et al., 2017). Most animal and fungal genomes contain only one *Thg1* copy encoding a simple Thg1 protein characterized by the catalytic and the C-terminal domains. By contrast, Arabidopsis contains two *ICA*/*Thg1* genes, each encoding two complete Thg1 units connected by a 40-amino acid peptide, which indicates that several duplication events have occurred during Arabidopsis *ICA*/*Thg1* evolution (Placido et al., 2010; Zhu et al., 2015). However, the overall evolution, including copy number and structure, for this conserved protein family remains unknown in plants.

Understanding the functional relationships between duplicated genes is fundamental for elucidating many biological processes because gene duplication has been a chief mechanism to generate genetic diversity during plant evolution (Panchy et al., 2016; Soltis and Soltis, 2016). The particular functional relationships between duplicated genes have led to different types of genetic interactions or epistasis, which underlie the gene networks regulating phenotypic diversity (Phillips, 2008). Multiple approaches are currently being used to address the mechanisms that preserve duplicated genes by neofunctionalization or subfunctionalization and their genetic interactions (Lynch, 2007). These include intra- and interspecific genome-wide comparisons estimating diversity and differentiation rates (Lynch and Katju, 2004; Panchy et al., 2016), as well as functional analyses of duplicated genes using artificial genetic reconstructions (Hanikenne et al., 2008; Gallego-Bartolomé et al., 2010; Vlad et al., 2014). In addition, several studies have dissected the functions of natural alleles segregating in duplicated genes at the intraspecific level, which are presently shaping the evolutionary fate of duplication events (Kliebenstein et al., 2001; Kroymann et al., 2003; Kliebenstein, 2008; Caicedo et al., 2009; Vlad et al., 2010; Prasad et al., 2012; Trontin et al., 2014).

In this study, we addressed the genetic, functional, and evolutionary relationships between the pair of duplicated genes, *ICA2* and *ICA1*, in Arabidopsis. The strong, high temperature–specific growth defects of Don-0 accession revealed substantial natural variation at *ICA2*, which shows synergistic epistasis with *ICA1*. We characterized the functional bases of *ICA2* variation for several adaptive traits, such as growth and flowering time, in relation to ambient temperature. In addition, we inferred the role of *ICA2* in climate adaptation via association analyses with climatic factors. Finally, we determined the evolutionary patterns of *ICA*/*Thg1* copy number and structure across the plant phylogeny. These results shed light on the conservation of the *ICA*/*Thg1* genes during plant evolution, the maintenance of Arabidopsis *ICA* duplication in the Camelineae tribe, and the contribution of *ICA2* to intraspecific variation for thermal developmental plasticity in Arabidopsis.

RESULTS

Fine Mapping Reveals That the Don-0 Growth Defect Is Caused by Two Closely Linked, Epistatic Loci

Previous analysis of the growth defect in the Sij-4 × Col crossing population at high temperature showed that this defect is determined by a recessive allele mapping to a 37-kb interval in *ICA1*. By contrast, similar analysis of Don-0 × Landsberg *erecta* (L*er*) or Sij-4 × L*er* crosses could only locate *ICA1* to a large genomic region of ~400 kb because recombinant plants between markers inside this region did not yield clear results (Zhu et al., 2015). This suggested the presence of a potential genetic modifier within this ~400-kb mapping interval. To determine whether another locus near *ICA1* could contribute to the growth phenotype of the Don-0 × L*er* cross, we analyzed a family of 2200 plants segregating for this genomic segment (Figure 1). A total of 33 recombinant plants in the 400-kb region were isolated, which were classified as L*er*, Don-0, or segregating families according to the severe growth defect observed in the vegetative phase of the F_3 offspring grown at 28°C. The application of a genetic model with a single gene causing this phenotype led to inconsistent fine mapping from multiple recombinant classes (e.g., recombinant classes i and m in Figure 1B). In addition, we did not find recombinant plants showing intermediate phenotypes, but the strong growth defect was only present in recombinants carrying homozygous Don-0 alleles in almost the complete 400-kb region. These results suggest that the growth phenotype was caused by Don-0 recessive alleles in at least two linked loci with synergistic epistasis. In particular, two classes of recombinant genotypes showing disparate phenotypes (Figure 1B, recombinant classes a and g) allowed us to map two loci to adjacent genomic regions of 95 and 139 kb, as defined by the physical distance between the markers flanking the recombination events of these plants. Genotypic and phenotypic analysis of the selfed progeny from six recombinants between both loci (classes b, c, d and h, i, j in Figure 1B) showed that the L*er* and Don-0 alleles at these loci display significant epistasis at high temperature ($P < 0.001$). This interaction explained 59% of the phenotypic variance for rosette size measured at 28°C (Figure 1C). Therefore, natural variation in two closely linked and interacting genes, named *ICA1* and *ICA2*, accounts for the vegetative growth defect of Don-0. Furthermore, only 25% of the offspring from recombinant plants homozygous for *ICA1*-Don-0 alleles and heterozygous *ICA2*-Don-0/*ICA2*-L*er* displayed the high temperature growth defect (chi-square $P > 0.05$ for 3:1 segregation test). Genotyping of these offspring showed that heterozygous *ICA2* individuals had normal growth at 28°C, which indicates that a single copy of *ICA2*-L*er* is sufficient to restore normal growth at high temperature, that is, the *ICA2*-L*er* allele is dominant versus *ICA2*-Don-0.

ICA2 Encodes a Thg1 Homolog That Interacts with *ICA1*

At2g31580, which was previously demonstrated to carry natural loss-of-function mutations underlying *ICA1* in Don-0 and Sij-4 (Zhu et al., 2015), is located in the *ICA1* mapping interval. Analysis of the *ICA2* genomic region identified the *ICA1* homolog *At2g32320* located 291 kb from *ICA1* (Figure 1B). Since both genes encode Thg1-like proteins that share 86% identity, we hypothesized that *At2g32320* is *ICA2*. To evaluate this, we first analyzed the sequence of *At2g32320* in the four parental accessions. L*er* and Don-0 differed in 60 single-nucleotide polymorphisms and 16 small insertion/deletions across the gene, including eight missense mutations that mainly affect the catalytic and C-terminal domains of the first Thg1 unit (Figure 2A). By contrast, Col and Sij-4 showed similar protein structure to that of the Don-0 accession, explaining our ability to map *ICA1* into a smaller interval in the Sij-4 × Col cross (Zhu et al., 2015). In addition, these findings suggest that Don-0/Sij-4/Col At2g32320 protein is required for *ICA1* loss-of-function mutations to display the growth defect. To determine whether the genetic interaction between *ICA1*/*At2g31580* and *At2g32320* accounts for the high temperature growth defect, we generated artificial *ICA1* loss-of-function mutants in accessions encoding At2g32320 proteins similar to those of Don-0 or L*er*. To this end, the previously developed line *35S*:*amiR-ICA1*, carrying a microRNA that targets the last *ICA1* coding exon (Zhu et al., 2015), was crossed with nine accessions and F_1 plants were analyzed (Figure 1D). All F_1 lines had normal phenotypes at 21°C. However, at 28°C, all F_1 individuals derived from four accessions with Don-0-like At2g32320 showed the severe growth phenotype, whereas the F_1 plants from five other accessions encoding L*er*-like At2g32320 proteins grew normally. Therefore, the temperature-dependent growth defect caused by *ICA1* loss-of-function depends on the natural allele at *At2g32320.*

In contrast to *ica1* loss-of-function mutants, a T-DNA insertional mutant of *At2g32320* in the Col background showed no obvious growth defect during the vegetative or reproductive phase at different temperatures (Figures 1A and 2B; Supplemental Figure 1). Nevertheless, we could not identify a double mutant for *ICA1* and *At2g32320* from a large F_2 population of 2346 plants (Supplemental Figure 2). This result strongly suggests that the *At2g32320* T-DNA allele is not functional and that it interacts with *ica1-2* to cause lethality. To prove that *At2g32320* is *ICA2*, we obtained 16 independent homozygous transgenic lines carrying a 5.6-kb genomic construct with the coding and promoter regions of *At2g32320* from L*er* or Don-0 in the genetic background of a Col *ica1-2* loss-of-function mutant that carries a Don-0-like allele of *At2g32320* (Figure 2; Supplemental Figure 3). All of these lines

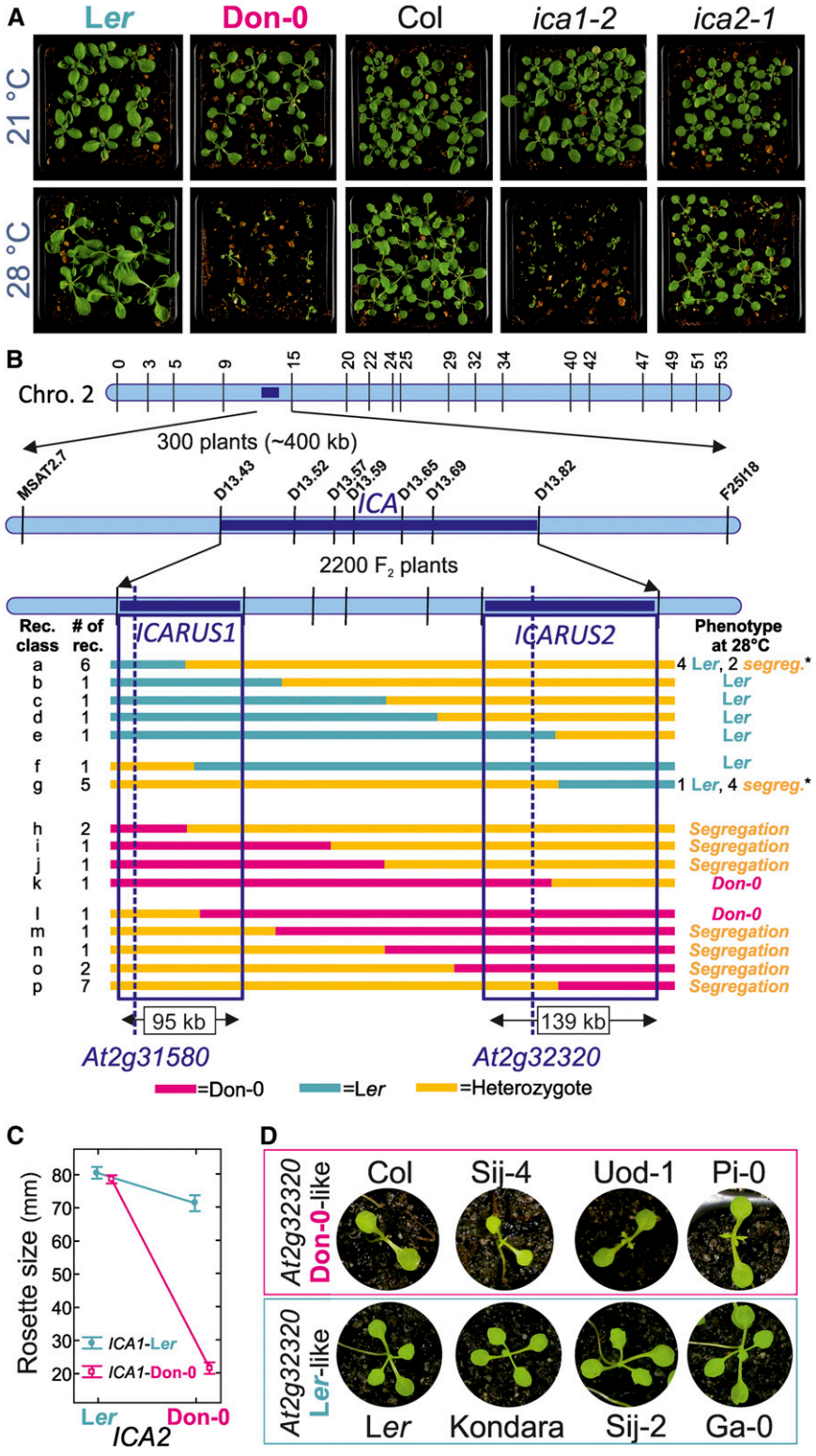

Figure 1. High Temperature Growth Defect and Fine Mapping of *ICARUS2*.

(A) Vegetative growth of 20-d-old L*er*, Don-0, Col, *ica1-2*, and *ica2-1* plants at 21 and 28°C.

(B) Genetic map of chromosome 2 and graphical genotypes of the different classes of Don-0/L*er* recombinant plants isolated in the ~400-kb genomic interval. Recombinants are classified and arranged according to Don-0/L*er* alleles in *ICA1* and *ICA2* genomic regions. The recombinant class (Rec. class)

showed normal growth at 21°C, similar to Col plants. However, they strongly differed at 28°C when we analyzed them in detail by measuring rosette diameter, flowering time, leaf number, and fruit length (Supplemental Table 1). Most of the lines with the *At2g32320* transgene from L*er* displayed growth and flowering phenotypes similar to those of the Col wild-type accession, indicating that this transgene fully complemented the phenotypic defects observed in *ica1-2* (Figure 2B). On the contrary, all but one of the eight lines with the *At2g32320* transgene from Don-0 showed phenotypes similar to *ica1-2* (small rosettes, late flowering, and small and sterile fruits) or intermediate between *ica1-2* and Col, which correspond to no and partial complementation, respectively. Overall, an *At2g32320* transgene from L*er*, but not from Don-0, complemented the growth defects produced by *ICA1* loss-of-function alleles, which is in agreement with the observed epistasis between L*er* and Don-0 alleles at *ICA1*/*ICA2* (Figure 1C). Hence, we concluded that *ICA2* is *At2g32320* and that the temperature-dependent developmental phenotypes of the Don-0 accession are caused by natural alleles in two homologous genes encoding Thg1 proteins.

Natural Variation at *ICA2* Affects the Cell Cycle and Sensitivity to DNA Damage

To determine whether *ICA2* is involved in the same cellular processes that were previously described for *ICA1* (Zhu et al., 2015), we also analyzed *ICA2* transgenic and mutant lines for cellular DNA content and sensitivity to DNA damage. Flow cytometry measurements showed that Don-0 and *ica1-2* plants contained larger proportions of cells with high ploidy levels than the wild-type L*er* and Col at 28°C, but not 21°C (Figure 2C; Supplemental Figure 4). By contrast, the DNA content profiles of *ica2-1* plants were similar to those of Col at both temperatures. In addition, at 21°C, *ica1-2* transgenic lines carrying *ICA2*-L*er* or *ICA2*-Don-0 alleles did not differ in terms of DNA content patterns (Supplemental Figure 4). However, both types of lines differed significantly at 28°C, since the *ICA2*-L*er* transgenic lines were similar to Col, whereas lines with *ICA2*-Don-0 transgenes displayed larger proportions of cells with 16C and 32C ploidy levels (chi-square $P < 0.001$), as observed for *ica1-2* (Figure 2C).

We measured sensitivity to DNA damage in the plants using the first leaf assay, which is based on growth arrest of the first pair of leaves in response to treatment with the DNA damaging agent Bleocin (BLEO) at 21°C (Rosa et al., 2013; Zhu et al., 2015). This assay showed that Don-0 and *ica1-2* were significantly more sensitive to BLEO damage than Col and L*er*, but no significant difference was found between *ica2-1* and Col plants (Figure 2D). On the contrary, both types of *ica1-2* transgenic lines differed significantly in terms of sensitivity to DNA damage ($P < 0.001$), since lines carrying *ICA2*-L*er* transgenes showed similar proportions of plants with true leaves after BLEO treatment to Col (89.2% ± 1.1%), whereas lines with *ICA2*-Don-0 had lower values (53.8% ± 1.9%), like *ica1-2* (Figure 2D). Thus, the effects of *ICA1* on both cellular traits depended on the *ICA2* allele, indicating that *ICA2* also interacts with *ICA1* for the regulation of cell division and for the capacity to repair DNA damage.

The Phenotypic Effects of *ICA2* Are Not Caused by *cis*-Regulatory Polymorphisms

Since natural alleles of *ICA2* differ in terms of mutations in the coding and noncoding gene regions, we aimed to find out whether the functional differences between Don-0 and L*er* could be explained by structural or *cis*-regulatory polymorphisms. We analyzed *ICA2* expression in the Don-0 and L*er* parental accessions, but no significant difference was detected (Figure 2E). We then quantified *ICA2* expression at 28°C in all lines carrying *ICA2* transgenes from Don-0 or L*er* in the *ica1-2* loss-of-function background (Figure 2F). On average, transgenic lines with *ICA2*-L*er* and *ICA2*-Don-0, which differ strongly in their developmental and cellular phenotypes, did not differ significantly in terms of *ICA2* expression ($P = 0.33$). This result indicates that natural alleles of *ICA2* do not bear *cis*-regulatory mutations affecting the overall gene expression level, as both parental transgenes included their own native promoters and untranslated regions. Therefore, the functional and phenotypic variation between natural alleles of *ICA2* in Don-0/Col and L*er* is likely caused by structural polymorphisms. Nevertheless, independent lines carrying the same transgene showed up to fivefold differences in expression ($P < 10^{-5}$). The *ICA2*-Don-0 line with the highest expression level was the only line with this transgene displaying almost full complementation (Figures 2B and 2F). On the contrary, the transgenic line with nearly the lowest *ICA2*-L*er* expression level showed the weakest complementation. Accordingly, significant correlations were detected between *ICA2* expression and the three quantitative traits affected by *ICA2* (Figure 2F). These results demonstrate that both natural alleles of *ICA2* encode functional proteins, but the L*er* allele is more active than the Don-0 allele. In addition, between-line variation in *ICA2* expression (due to the different transgene insertion sites) also affects *ICA2* function and growth at high temperature.

Figure 1. (continued).

and the number of independent recombinant plants with similar genotype analyzed (# of rec.) is shown in the left side of the panel. The 28°C growth phenotype of the offspring derived from each recombinant was recorded as L*er*, Don-0, or segregating families and is presented in the right side of the panel. The two most informative classes of recombinants are marked with asterisks (*). They corresponded to genotypes shared by multiple independent recombinants but displaying disparate growth phenotypes, as indicated on the right. The size and location of *ICA1* and *ICA2* mapping intervals, delimited by the markers flanking the recombination events of these two classes of genotypes, are depicted with dark blue rectangles. The positions of the pair of duplicated genes *At2g31580* and *At2g32320* are indicated with dark blue dashed lines. Chro. 2, chromosome 2.

(C) Genetic interaction between *ICA1* and *ICA2* in the L*er*/Don-0 mapping population. Panel shows the 28°C rosette size (mean ± SE of 14 to 25 plants) of homozygous plants for L*er* or Don-0 alleles at *ICA1* and *ICA2* regions.

(D) The 28°C growth phenotypes of 14-d-old F_1 plants derived from crosses between Col line *35S:amiR-ICA1* and accessions carrying a Don-0 (top panel) or L*er*-like (bottom panel) allele at *At2g32320*.

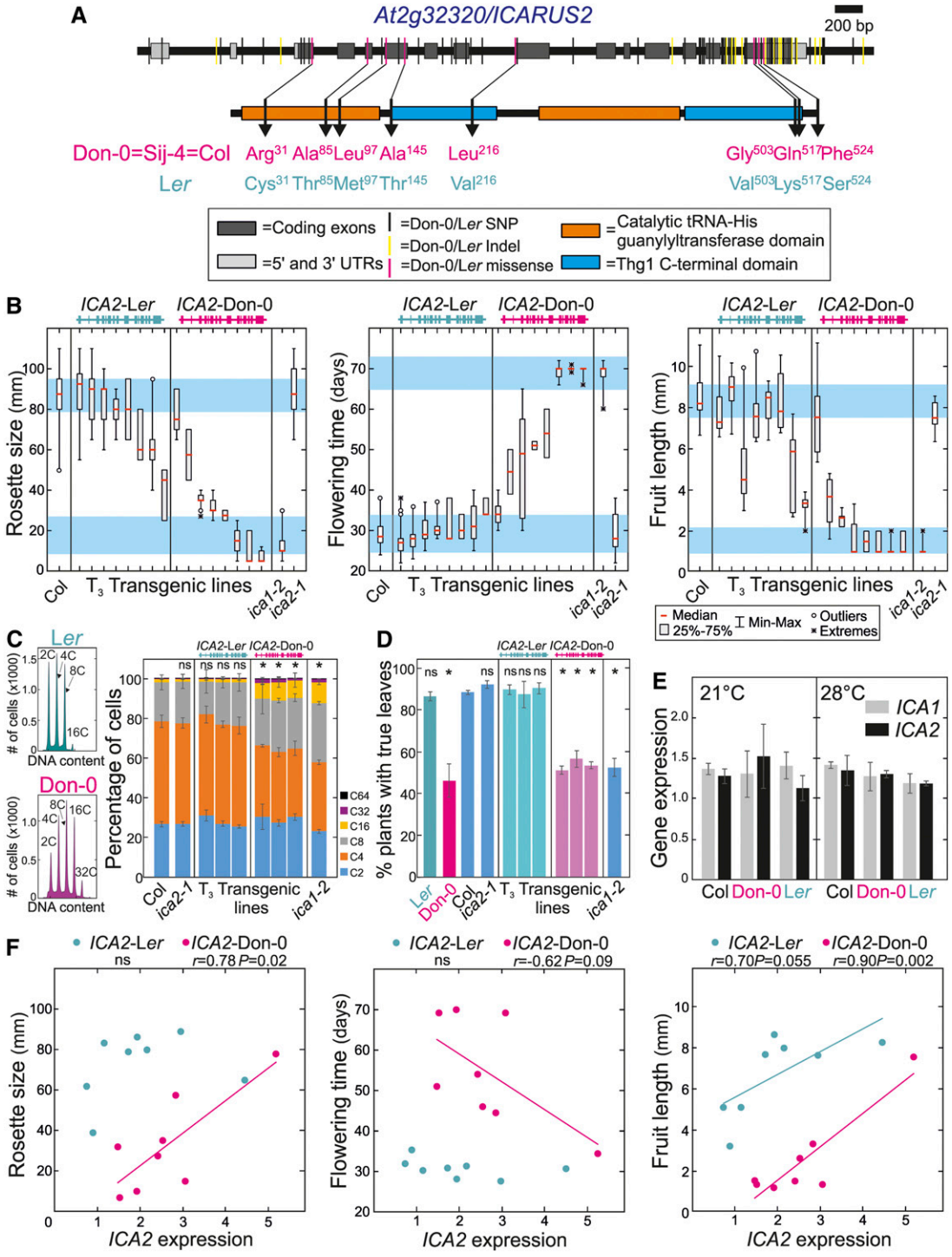

Figure 2. Genetic Complementation of Developmental and Cellular Traits by Natural Alleles of *ICA2*.

(A) Genomic and protein structure of *ICA2* from parental accessions (L*er*, Don-0, Sij-4, and Col) showing protein domains and missense mutations. SNP, single-nucleotide polymorphism; UTRs, untranslated regions.

(B) Phenotypic analyses of *ica1-2* homozygous transgenic lines carrying *ICA2*-L*er* or *ICA2*-Don-0 grown at 28°C, for rosette size (left panel), flowering time (middle panel), and fruit length (right panel). Transgenic lines in the various panels are arranged in the same order. Upper and lower 95% confidence intervals for Col and *ica1-2* phenotypes are shown as blue-shaded areas.

Natural Variation in *ICA2* Affects Growth at Different Temperatures

To characterize the effects of *ICA2* allelic variation in the presence of active *ICA1* alleles, we also analyzed 13 independent homozygous transgenic lines carrying Don-0 or L*er* *ICA2* transgenes in the *ica2-1* genetic background. Quantitative analysis of leaf size traits at different temperatures showed that at 28°C, but not 21°C, *ica2-1* had smaller petioles and blade length or area than Col ($P < 0.01$), indicating that *ICA2* weakly but significantly affects the thermomorphogenic response (Figure 3). In addition, homozygous lines for *ICA2*-L*er* and *ICA2*-Don-0 transgenes differed in terms of leaf size traits at both 21 and 28°C ($0.001 < P < 0.02$; Supplemental Table 1). On average, the *ICA2*-L*er* plants had larger leaf petioles and blades than *ICA2*-Don-0 plants (Figures 3A, 3B, and 3C), again pointing out that the *ICA2*-L*er* allele is more active than *ICA2*-Don-0. Parallel analyses of flowering time at different temperatures showed that neither the *ica2-1* mutation nor *ICA2* transgenes had a significant effect on this trait ($P > 0.05$). However, all transgenic lines displayed accelerated flowering mediated by high temperature similar to Col ($P < 0.001$; Figure 3D). Therefore, natural variation in *ICA2* did not affect flowering time in an active *ICA1* genetic background.

To quantify the effects of temperature and *ICA2* alleles on gene expression, we also analyzed *ICA2* and *ICA1* mRNA levels in all of these lines. Most of the transgenic lines had higher *ICA2* expression levels than the Col parental accession, although there was substantial variation among lines (Figure 3E). Overall, no significant difference in expression was detected between *ICA2* transgenes ($P = 0.8$). By contrast, a small effect of temperature on *ICA2* expression was detected, which depended on the transgene, because two lines carrying *ICA2*-L*er* showed lower expression at 28 versus 21°C (Figure 3E). These results suggest that the position of the *ICA2* transgene insertion affects the temperature response of the transgene. In addition, *ICA1* expression showed much lower variation among transgenic lines, and no significant difference was found between transgenes at both temperatures (Figure 3F).

ICA2 Diversity Shows Broad Geographic Distribution and Climatic Association

To determine the intraspecific relevance of the structural polymorphisms of *ICA2* found in Don-0 and L*er*, we analyzed the global diversity of *ICA2* in Arabidopsis (1001 Genomes Consortium, 2016). Clustering analysis of 791 sequences identified two major haplogroups present in 73% and 15% of the worldwide accessions corresponding to the Don-0/Col and L*er* alleles, respectively (Figure 4A). Both haplogroups differed in the eight Don-0/L*er* polymorphic amino acids and in numerous polymorphisms in introns and the 3′ region, which displayed moderate-to-strong linkage disequilibrium. Network analyses of protein sequences showed that the ICA2-Don-0/Col haplogroup is closer to the *A. lyrata* haplotype and, consequently, to the ancestral allele, whereas ICA2-L*er* is the most distant allele (Figure 4B).

Geographic analyses of *ICA2* diversity revealed a strong spatial structure, as accessions with the L*er* haplogroup are mainly distributed in Northern Europe and Asia (Figure 4C). Approximately 90% of the ICA2-L*er* accessions belonged to genetic groups 3, 5, and 6 established from genome sequences (1001 Genomes Consortium, 2016), which are only found in Scandinavia and Asia. To further examine whether the distribution of ICA2 haplogroups is related to climate, we also tested associations using climatic data from the original population locations (Figure 4C). Analyses of all 687 accessions with L*er* or Don-0/Col haplogroups detected significant associations of ICA2 with temperature seasonality and isothermality on a global scale ($P < 0.008$). Moreover, since the strong genetic structure of the worldwide collection might mask or confound climate associations, we performed similar tests including only the 159 accessions of genetic groups 3, 5, and 6, finding similar results at $-\log(P) = 5.3$. Overall, it appears that the ICA2-L*er* haplogroup is mainly distributed in locations with moderately low temperature seasonality and isothermality, whereas the ICA2-Don-0/Col haplogroup showed a wider climatic distribution. Thus, demographic and climatic factors linked to annual and daily fluctuations in temperature likely contributed to the current geographic distribution of ICA2 haplogroups.

Interspecific *ICA*/*Thg1* Gene Diversity across the Plant Phylogeny Discloses Ancient Gene Duplications and Rearrangements

To explore the evolution of the Arabidopsis complex locus including both *ICA1* and *ICA2*, we analyzed the number, structure, and physical positions of *ICA* genes in the well-annotated genomes available for 58 species across the phylogenetic tree of green plants (Figure 5). Overall, most diploid species carried only one or two *ICA*/*Thg1* genes, encoding proteins with an average identity of 60.1% ± 13.4%, which indicates a strong conservation

Figure 2. (continued).

(C) Flow cytometry analyses of nuclear DNA content in parental, transgenic, and mutant lines grown at 28°C. Left panel shows representative ploidy profiles of L*er* and Don-0 leaves. Right panel displays the percentage of leaf cells with 2C to 64C ploidy levels in six transgenic lines carrying *ICA2*-L*er* or *ICA2*-Don-0 transgenes compared with Col, *ica1-2*, and *ica2-1* genotypes.

(D) Sensitivity to DNA damage measured by the first leaf assay in 10-d-old seedlings treated with BLEO. The percentage of BLEO-treated plants with true leaves is shown in relation to mock samples for parental, mutant, and *ica1-2* transgenic lines. In **(C)** and **(D)**, each bar represents the mean ± SE of three biological replicates, and statistical comparisons of each line and Col are indicated on the bars.

(E) *ICA1* and *ICA2* expression in parental accessions at different temperatures. Each panel shows the mean ± SE of three biological replicates.

(F) Correlations between *ICA2* expression and rosette size (left panel), flowering time (middle panel), and fruit length (right panel) in *ICA2* transgenic lines grown at 28°C. The expression of each line is relativized to that of untransformed Col plants. Statistical significances of Pearson correlation coefficients and significant regression lines are shown in each panel. ns, nonsignificant; *$P < 0.001$.

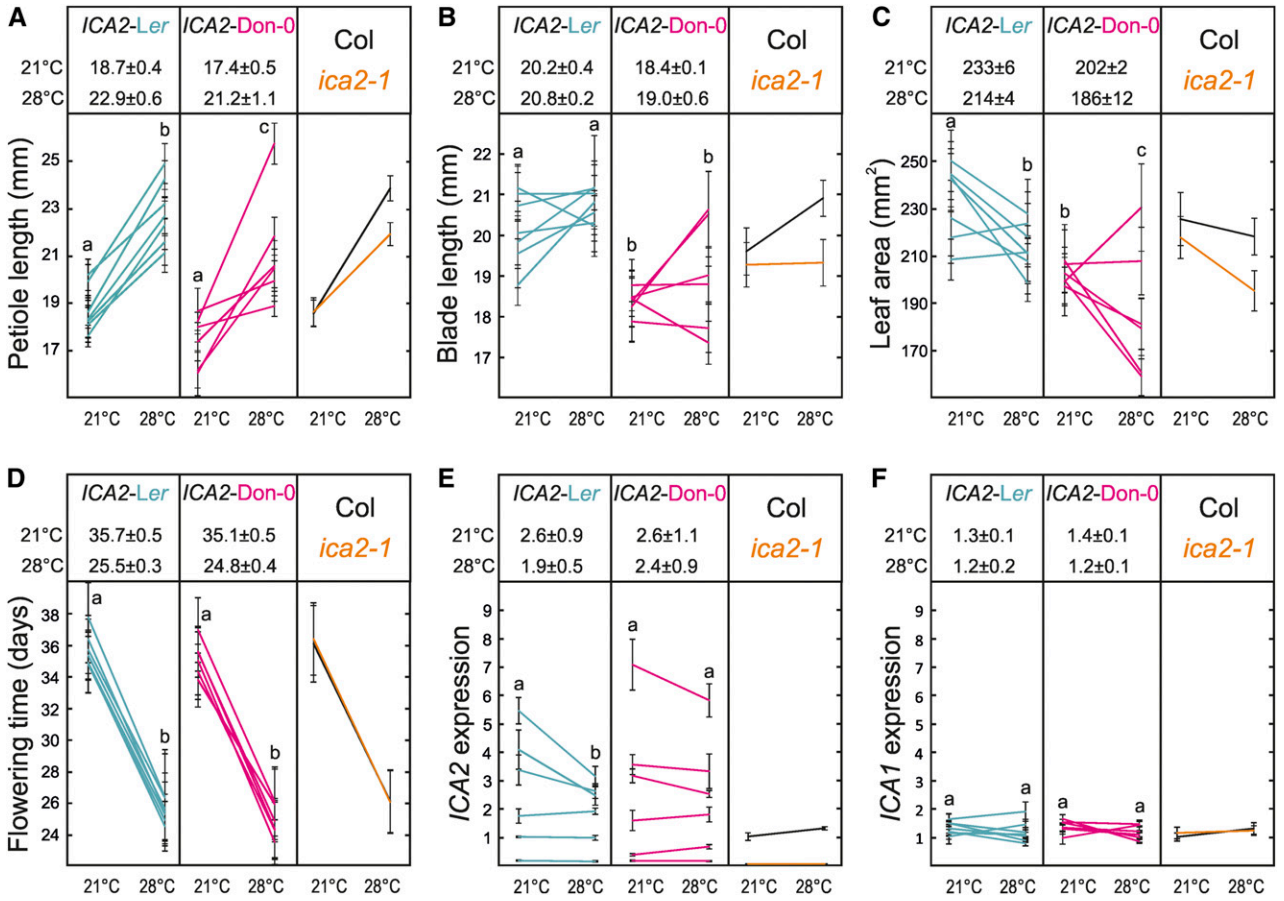

Figure 3. Phenotypic Effects of *ICA2* Natural Alleles at Different Ambient Temperatures.

(A) to **(D)** Reaction norms of *ica2-1* homozygous transgenic lines carrying *ICA2* transgenes from L*er* (left panel) or Don-0 (middle panel), as well as Col and *ica2-1* control lines (right panel), for petiole length **(A)**, blade length **(B)**, leaf area **(C)**, or flowering time **(D)** estimated at 21 and 28°C.
(E) and **(F)** Expression of *ICA2* **(E)** and *ICA1* **(F)** in the same transgenic and control lines. In **(A)** to **(D)**, panels show the mean ± SE of each line derived from 20 to 30 plants grown at 21 or 28°C. In **(E)** and **(F)**, panels show the mean ± SE of each line grown at 21 or 28°C as estimated from three technical replicates. Values of all lines are relative to Col expression at 21°C. The effects of *ICA2* transgene and temperature were statistically tested by mixed-model analysis of variance. In each panel, the same or different letters close to the four groups of lines (two transgenes and two temperatures) indicate non-significant and significant differences, respectively, as tested by Tukey's test ($P < 0.05$).

of the low number and structure of *ICA* genes during plant evolution. As described for most fungi and animal species, the oldest clades of Chlorophyta and Embriophyta carry only one *ICA* gene encoding a single Thg1 unit (simple *ICA/Thg1* gene). By contrast, the moss *Spagnum fallax*, the basal group of Tracheophyta (*Selaginella moellendorffii*), and the early diverging monocots (*Zostera marina*) and eudicots (*Aquilegia coerulea*) carried two or three gene copies, indicating that a first duplication of the simple *ICA/Thg1* gene occurred in an ancestral tracheophyte ~450 million years ago (Mya; Vargas and Zardoya, 2014). Furthermore, *ICA* genes from all analyzed grass monocots and core eudicots encode proteins with two Thg1 units, which we refer to as double *ICA/Thg1* genes (Figure 5). Therefore, the transition from simple to double *ICA/Thg1* genes could be dated to the diversification of mono- and dicotyledonous plants ~120 Mya (Vargas and Zardoya, 2014). We also performed maximum-likelihood (ML) phylogenetic analysis of ICA/Thg1 proteins, which, as expected, reflected the overall phylogeny of green plants from a common ancestor with fungi and animals (Figure 6A). However, this analysis did not detect groups of orthologous genes supporting a common ancestral duplication in different early diverging monocots and eudicots with at least two copies of the simple *ICA/Thg1* gene (*Z. marina*, *Musa acuminata*, and *A. coerulea*); instead, all proteins of each species clustered together. This finding suggests that multiple independent duplications of the *ICA/Thg1* simple gene might have occurred in those basal groups and/or that both copies of *ICA/Thg1* genes co-evolved in these plants to maintain high similarity.

Plants of most core eudicot families carried only one double *ICA/Thg1* gene, with the main exception being some recent polyploid species, such as soybean (*Glycine max*) and apple tree (*Malus domestica*), which had larger numbers of these genes. However, 9 of 11 analyzed Brassicaceae plants had two or more genes, pointing to specific *ICA/Thg1* duplications in this family. In particular, Arabidopsis, *Arabidopsis lyrata*, *Capsella rubella*, and

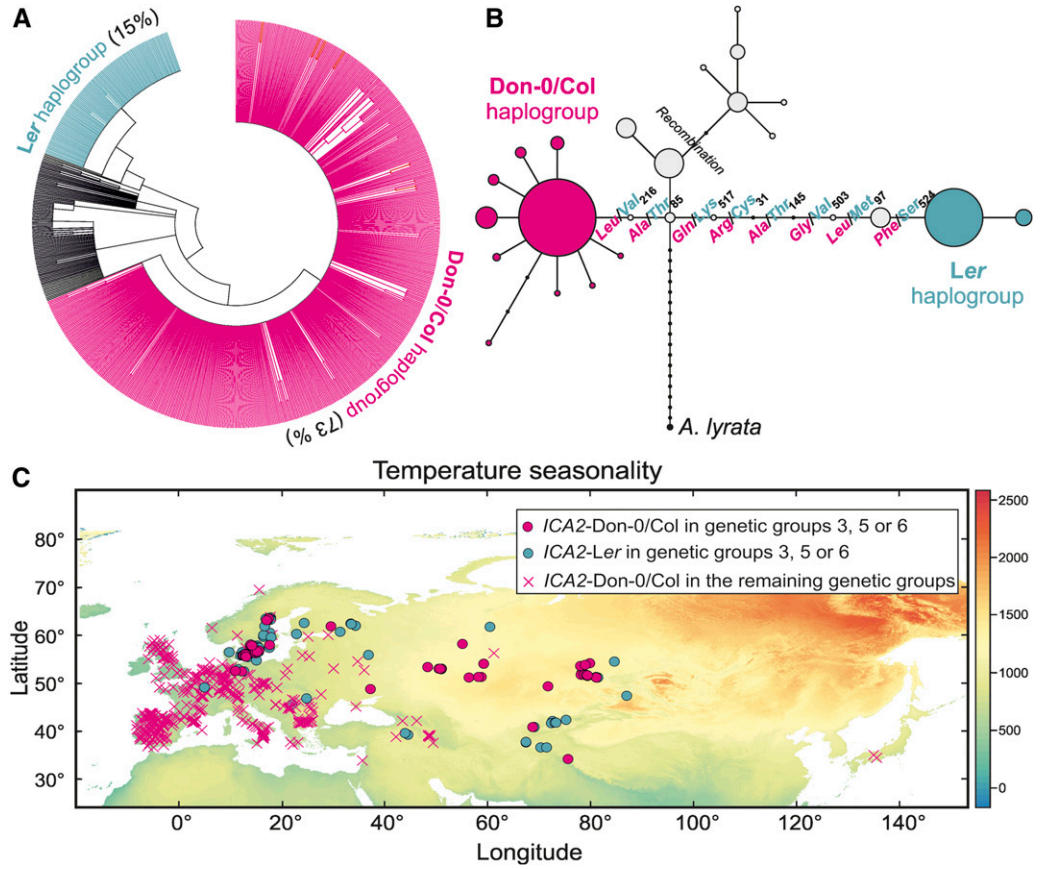

Figure 4. Genetic Diversity and Geographic and Climatic Distribution of *ICA2* in Arabidopsis.

(A) Neighbor-joining tree showing the genetic relationships among 791 *ICA2* worldwide genomic sequences. Branches corresponding to partitions reproduced in <50% bootstrap replicates are collapsed.
(B) Haplotype network of ICA2 proteins from worldwide accessions of Arabidopsis and *A. lyrata*. Each node corresponds to an amino acid substitution, with black dots corresponding to predicted nodes that are not present in the analyzed sequences. Areas of nodes are proportional to frequency.
(C) Geographical and climatic distribution of major ICA2 haplogroups in Eurasia. Temperature seasonality is measured as the SD of monthly temperature averages (units of the scale are degrees Celsius × 100). In **(A)** to **(C)**, accessions and amino acids belonging to Don-0/Col or L*er* haplogroups are shown in magenta and sea green, respectively.

the hexaploid *Camelina sativa*, all belonging to the Camelineae tribe, contained one to three pairs of *ICA/Thg1* genes closely linked at physical distances smaller than 1 Mb (Figures 5 and 6). The similar arrangement of most genes within *ICA* intervals of these species revealed strong microsynteny and common ancestry for the *ICA* genomic region of Camelineae (Figures 6B and 6C; Supplemental Figure 5). In addition, diploid and polyploid species of the Brassiceae tribe also contained multiple *ICA/Thg1* copies, but these were located on different chromosomes. The ML phylogenetic analysis showed that the first cluster separating in the Brassicaceae family includes ICA2 from Arabidopsis and half of the ICA proteins from other Camelineae species (Figure 6A). Moreover, all ICA/Thg1 sequences from the Brassiceae tribe clustered together with Arabidopsis and other Camelineae ICA1 proteins. Therefore, two independent *ICA/Thg1* duplications have occurred within the Brassicaceae family, but only the older duplication of Camelineae maintained the close linkage of the two *ICA/Thg1* genes.

DISCUSSION

Genetic Interactions among Natural Alleles Uncover a Conserved Function for the Duplicated *ICARUS* Genes in Arabidopsis

The genetic and functional analyses performed in this study show that the pair of duplicated genes *ICA1* and *ICA2* of Arabidopsis behaves as a rather complex locus, since both genes are closely linked in the genome and their natural alleles interact to produce a severe growth defect that is conditional upon high ambient temperature. This locus illustrates the extreme complexity that genetic and functional relationships between duplicated genes can achieve in plants. Most previous analyses addressing the function of natural alleles in duplicated genes have focused on recent duplications segregating within a single species and mainly affecting tandemly repeated genes (Kliebenstein et al., 2001; Kroymann et al., 2003; Caicedo et al., 2009; Prasad et al., 2012;

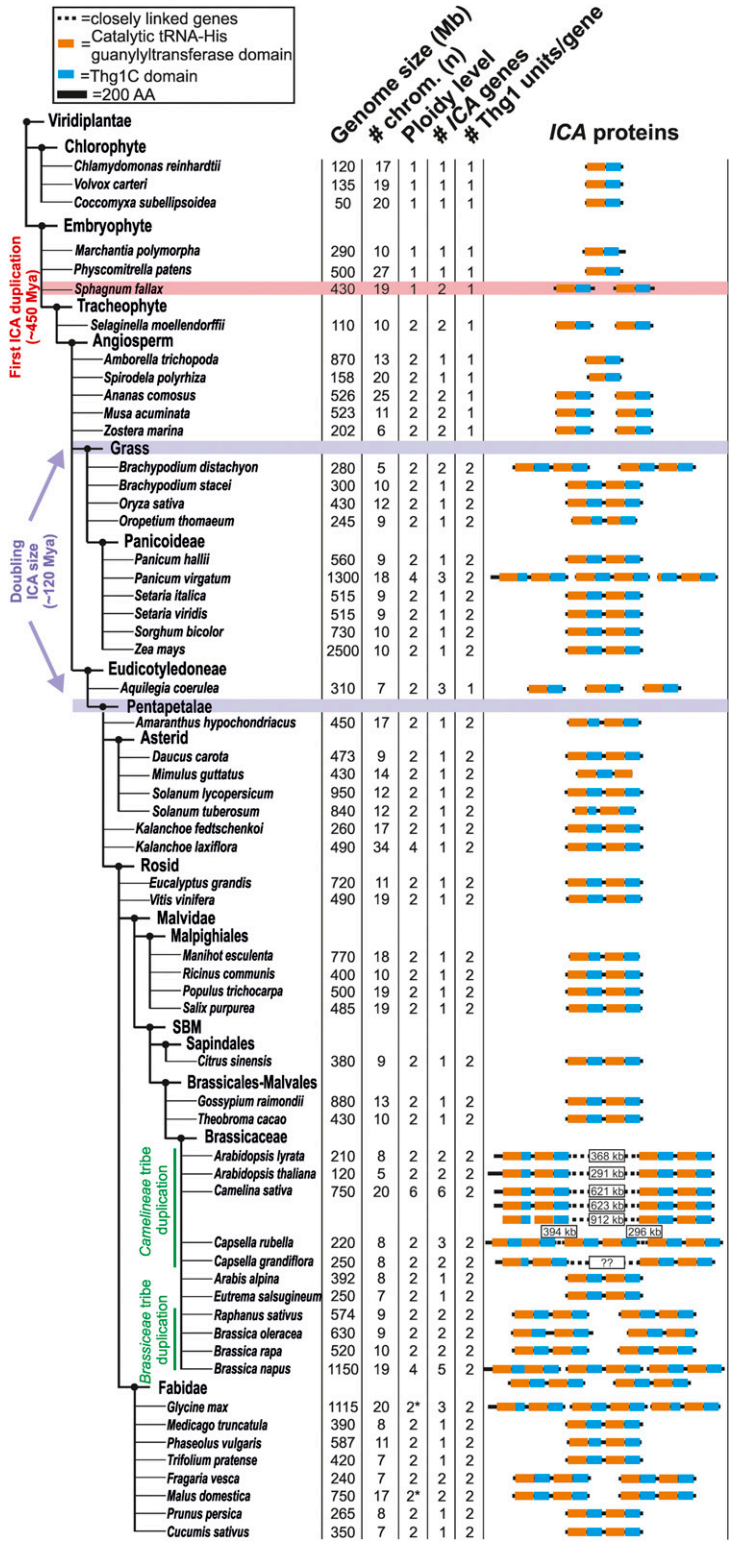

Figure 5. Evolution of the Number and Structure of ICA Proteins in Viridiplantae.

Sizes and domain structures of proteins encoded by *ICA* genes present in the genomes of 58 plant species are depicted in the right part of figure. For each species, the genome size, chromosome number, ploidy level of the dominant phase of the life cycle, number of *ICA* genes per haploid genome, and number of Thg1 units encoded per gene are also shown. Ploidy level indicated as 2* corresponds to species evolved by recent polyploidization. Species are arranged

Trontin et al., 2014; see Vlad et al., 2010 as nontandem repeat duplication). However, Arabidopsis *ICA* duplication is conserved across the Camelineae tribe of Brassicaceae, providing an example of the natural variation in older duplications, which have been mainly approached in terms of inter- and intraspecific hybrid incompatibilities (Bomblies et al., 2007; Bikard et al., 2009; Alcázar et al., 2010, 2012; Bomblies, 2010).

Phenotypic analyses of plants carrying different natural alleles at *ICA1* and *ICA2* show that *ICA2*-Don-0/Col is the recessive allele and that only homozygous plants for recessive alleles at both *ICA* genes display severe developmental defects along the Arabidopsis life cycle, specifically at high temperature. This synergistic, double dominant epistasis between *ICA1* and *ICA2* indicates that both genes are involved in the same biological process, because no additional or intermediate phenotypes were observed in heterozygous plants for each *ICA* gene or in homozygous plants for the recessive allele only in one of the two genes. The genetic interaction affected not only plant growth and flowering traits but also cellular phenotypes, such as the high nuclear cell content caused by endoreduplication and the sensitivity to DNA damage. These results demonstrate that the temperature-dependent phenotypes previously described for *ICA1* (Zhu et al., 2015) are determined by the genetic interaction between both *ICA1* and *ICA2* genes. Therefore, *ICA2* is also involved in regulating the cell cycle and cell division to modulate cell size and subsequently plant growth, mainly at high temperature. Hence, in contrast to the many duplicated genes that have diverged from each other by subfunctionalization or neofunctionalization (Lynch, 2007), *ICA1* and *ICA2* have a general conserved function in Arabidopsis.

The characterization of the epistasis between *ICA1* and *ICA2* in the regulation of plant growth at high temperature provides additional functional information about these genes. First, both Don-0 and L*er* natural alleles of *ICA2* are active, but *ICA2*-L*er* is dominant and a gain-of-function allele, as shown by the analysis of transgenic lines in the *ica1* and *ica2* backgrounds. Second, the differential behavior of artificial loss-of-function mutations of *ICA1* and *ICA2* genes points to the major relevance of *ICA1* for growth at high temperature, although only in the background of the most frequent and weaker *ICA2*-Col allele. Third, concordant with the lethality of null mutants described in yeast (Gu et al., 2003), the combination of null alleles in both *ICA* genes is likely to be lethal in Arabidopsis, as we could not obtain an *ica1-2 ica2-1* double mutant.

In agreement with the functional conservation observed in Arabidopsis, *ICA* genes show very limited divergence over hundreds of million years, as the number, structures, and sequences of ICA proteins appeared highly conserved across the plant phylogeny. Two major ancient structural events have occurred during plant evolution. The first duplication of the simple *ICA* gene encoding a single Thg1 unit took place at the origin of tracheophyte plants ~450 Mya (Vargas and Zardoya, 2014). Second, with the early divergence of monocots and eudicots ~120 Mya, either the two simple *ICA*/*Thg1* genes were rearranged, or one of them was duplicated in tandem and the other lost, to render a single gene encoding two Thg1 units. The evolution of such a double *ICA*/*Thg1* gene ensured that both Thg1 units display similar expression and protein stoichiometry. The presence of one double *ICA* gene has been maintained throughout most angiosperms, with the main exception being Brassicaceae, where we detected two independent duplications that occurred in the ancestors of the Camelineae and Brassiceae tribes. Taking into account our current view of the evolution of Brassicaceae, these *ICA* duplications can be dated to the Middle Miocene, ~12 to 18 Mya (Huang et al., 2016), although ML phylogenetic analysis supports the notion that the Camelineae duplication is older than that of the Brassiceae. Thus, *ICA* genes appear to comprise a very small gene family well suited for phylogenomic studies across the plant kingdom because they are universal, essential, and rather conserved.

Natural Structural Variation in *ICARUS2* Is Likely Involved in Growth Adaptation to Temperature Fluctuations

In contrast to *ICA1*, for which various independent and very low frequency loss-of-function mutations have been found in nature (Zhu et al., 2015), the natural gain-of-function allele of *ICA2* described here shows a high worldwide frequency. Our molecular and environmental characterizations provide several clues about the functional bases of natural variation in *ICA2* and its role in the adaptation of Arabidopsis to climate. On one hand, the phenotypic behavior and gene expression of *ICA2* transgenic lines at different temperatures indicate that the functional difference between Don-0/Col and L*er* alleles is likely caused by one or several amino acid substitutions affecting ICA2 structure. Considering that Thg1 proteins from bacteria, animals, and fungi function as tetramers to catalyze the addition of a single G nucleotide to the 5′ end of the $tRNA^{His}$ (Heinemann et al., 2012; Lee et al., 2017), we hypothesize that structural mutations in ICA2 in Arabidopsis might alter the interactions among Thg1 units and/or the catalytic activity of the protein complex. Supporting this hypothesis, the amino acid substitution Arg-31 to Cys-31 found in ICA2 is located in the activation site of ICA/Thg1 proteins, which binds to a GTP molecule through the activation pocket formed by amino acids 29 to 37 (Lee et al., 2017). Nevertheless, we cannot exclude the possibility that natural alleles of *ICA2* might also differ in terms of the precise cellular and temporal regulation of gene expression or in transcript splicing, because artificial modification of *ICA2* expression levels showed significant phenotypic effects.

On the other hand, the natural variation in *ICA2* affects growth mainly at high temperature, hence contributing to the variation in plasticity in relation to temperature. This is reflected by the severe growth defect displayed only at high temperature by plants harboring loss-of-function alleles in both *ICA* genes. Also, the *ica2-1*

Figure 5. (continued).

according to the plant phylogeny as established in Phytozome (http://phytozome.jgi.doe.gov). Major *ICA* duplications or gene size doubling are indicated in red or purple, respectively, in the left side of the panel. Main tribes of Brassicaceae carrying *ICA* duplications are indicated in green. *ICA* genes that are closely linked in the same chromosomes are depicted as connected by a dashed line, indicating the size of the DNA genomic interval between them. chrom., chromosomes.

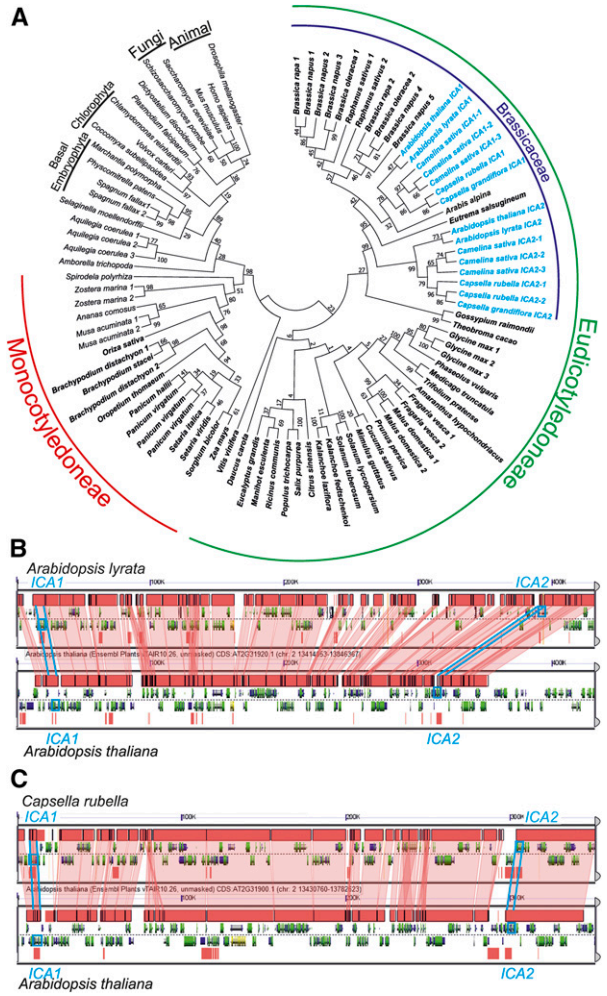

Figure 6. Evolutionary and Microsynteny Relationships of *ICA1* and *ICA2* in Brassicaceae.

(A) ML phylogenetic tree obtained for 94 ICA proteins from 58 species across the plant phylogeny and seven model organisms from other life kingdoms, as described in Figure 5. The bootstrap consensus tree inferred from 1000 replicates is taken to represent the evolutionary history of the taxa analyzed (Tamura et al., 2011). Double and simple ICA proteins detected by the genome and protein structure analysis described in Figure 5 are shown with bold or normal text, respectively. For the five Brassicaceae species belonging to the Camelineae tribe and carrying multiple *ICA* genes (shown in light blue), ICA proteins are named by adding *ICA1* or *ICA2* to the species name based on their closer relationship to ICA1 or ICA2 from Arabidopsis. For the remaining plant genomes with more than one *ICA* gene, ICA proteins are named by adding a number from one to three to the species name. Red and green depict mono- and dicotyledonous clades, respectively, whereas dark blue spans the Brassicaceae plant family.
(B) and **(C)** Microsynteny within *ICA1/ICA2* genomic region between *A. lyrata* **(B)** or *C. rubella* **(C)**, and Arabidopsis. Microsyntenic blocks are shown as red rectangles above the coding sequences connected by shaded lines. The positions of *ICA1* and *ICA2* are framed in blue. Microsynteny analyses were performed using the Web-based SynMap browser as implemented in the Comparative Genomics CoGe platform (https://genomevolution.org/coge/; Lyons and Freeling, 2008; Haug-Baltzell et al., 2017).

mutant and *ICA2* natural variants affect relevant traits targeted by high temperature, such as leaf size, in the presence of functional *ICA1* alleles. These phenotypes suggest that *ICA2*-Don-0/Col increases thermomorphogenesis and leaf growth plasticity. In addition, the more active *ICA2*-L*er* allele also accelerates flowering initiation compared with *ICA2*-Don-0 when combined with *ICA1* loss-of-function alleles at high temperature. Most likely, the strong flowering time effect caused by *ICA1* and *ICA2* interaction in the *ica1* background underlies a large-effect quantitative trait locus previously identified specifically at 28°C in an experimental Don-0/L*er* population (Méndez-Vigo et al., 2016). This effect is not only a consequence of the potential developmental delay produced by the severe growth defect, because the *ica1-2* mutant and lines carrying *ICA2*-Don-0 transgenes in the *ica1-2* background exhibited delayed flowering, but also developed more leaves than the wild type (Supplemental Figure 3B). Interestingly, this quantitative trait locus has been shown to genetically interact with the flowering integrator *FLC*, which also affects the thermal plasticity of flowering (Méndez-Vigo et al., 2016). Thus, *ICA2* and *ICA1* appear to be a pair of molecular components that contribute to the natural variation in the temperature-mediated regulation of leaf growth and flowering time.

The significant associations between ICA2 haplogroups and environmental variables related to the daily and annual fluctuations in temperature suggest that the natural variation in *ICA2* is involved in adaptation to these climatic factors. It must be emphasized that the strong growth defect caused by the *ICA1* and *ICA2* interaction has been shown to be quantitatively variable and reversible depending on temperature (Zhu et al., 2015). This further supports the notion that, under natural conditions, *ICA2* is likely more involved in regulating the cell cycle and plant growth in response to thermal fluctuations versus average temperatures. Nevertheless, deciphering the evolutionary processes that maintain the natural variation in *ICA2* awaits additional studies quantifying the fitness effects of *ICA2* in natural and/or fluctuating environments.

It remains unknown how Arabidopsis *ICA* genes affect growth and development differentially depending on ambient temperature. Various outcomes from the analyses of accessions and transgenic lines support the notion that this is not determined by the differential regulation of *ICA* expression. First, *ICA2* and *ICA1* did not show significant differences in expression, indicating a rather similar contribution of both genes at the transcriptional level. Second, *ICA2* and *ICA1* displayed comparable expression levels at 21 and 28°C, which implies that the growth defect caused specifically at high temperature is not a consequence of reduced expression of *ICA2* at 28°C. These results suggest that other proteins that interact with the ICA tetramer and show temperature-mediated transcriptional or posttranscriptional regulation might provide the temperature conditionality of the phenotypic effects of *ICA*. Favoring this view, Thg1 proteins from yeast and human have been shown to interact with the origin recognition complex involved in DNA replication and cell division (Rice et al., 2005) and with mitofusin 2, a fundamental component for mitochondria fusion (Edvardson et al., 2016). Alternatively, given the function of *Thg1* genes in $tRNA^{His}$ maturation (Heinemann et al., 2012; Lee et al., 2017), the temperature dependence of *ICA* might be determined through the regulatory functions mediated by uncharged

or modified tRNAs or the recently identified category of functional small RNAs derived from tRNAs, which have been shown to regulate gene expression under stress conditions (Heinemann et al., 2012; Raina and Ibba, 2014; Alings et al., 2015; Zhu et al., 2018). Currently, a large body of studies on tRNA biology have linked tRNA metabolism with the transcriptional and translational regulation of specific genes, as well as with cancer and other diseases, including the association of a human Thg1 mutation with cerebellar ataxia (Edvardson et al., 2016; Orioli, 2017). However, the relevance of such interactions and regulations is mostly unknown in plants, and further research is needed to elucidate the precise functional mechanisms underlying the universal *ICA/Thg1* genes.

METHODS

Plant Materials

The parental Arabidopsis (*Arabidopsis thaliana*) accessions Don-0, L*er*, Col, and Sij-4, as well as the loss-of-function T-DNA mutant *ica1-2* in the Col background, were described previously (Zhu et al., 2015). The T-DNA insertion mutant *ica2-1* in the Col background was obtained from Nottingham Arabidopsis Stock Centre (N680284) as line SALK_131808. A previously developed *35S*:*amiR-ICA1* line in the Col-0 background (Zhu et al., 2015) was used to silence *ICA1* in different wild accessions. This line was crossed with the following accessions: Col, Sij-4, Uod-1 (N6975), and Pi-0 (N7298) belonging to the *ICA2*-Don haplogroup and L*er*, Bd-0 (N7013), Ga-0 (N6919), Kondara (6929), and Sij-2 (N10009) in the *ICA2*-L*er* haplogroup. This artificial microRNA targets the *ICA1* sequence 5′-GGGAAG AACACCTACACTTC-3′, which is fully conserved among crossed accessions and absent in *ICA2* gene. The artificial microRNA was a single gene target, as shown by WMD3 (http://wmd3.weigelworld.org).

Fine mapping of *ICA1* and *ICA2* was performed using selfed progeny of 2200 plants obtained from the recombinant inbred line L*er*/Don-0-70 derived from a cross between the Don-0 and L*er* accessions (Méndez-Vigo et al., 2016). This line was heterozygous for a genomic region spanning the *ICA1* and *ICA2* loci but homozygous L*er* (60%) or Don-0 (35%) for the rest of the genome. Genetic markers developed for fine mapping are described in Supplemental Table 2.

The genetic interaction between L*er* and Don-0 alleles of *ICA1* and *ICA2* was tested by analyzing plants carrying the four genetic combinations that were homozygous L*er* or Don at these loci in an otherwise homogeneous background. These plants were obtained from the selfed progeny of six recombinants selected from the fine mapping population as heterozygous L*er*/Don-0 for *ICA2* and homozygous *ICA1*-L*er* (recombinants classes b, c, and d in Figure 1B) or *ICA1*-Don (recombinants h, i, and j in Figure 1B). Between 25 and 30 offspring plants from each recombinant were grown at 28°C, phenotyped, and genotyped with the markers developed for fine mapping (Supplemental Table 2). At least 14 offspring plants of each of the four homozygous genotypes were used for phenotypic comparison.

Growth Conditions and Phenotypic Analyses

Plants were grown in pots with soil and vermiculite at a 3:1 proportion in growth chambers supplemented with light to provide a long-day photoperiod (16 h of cool-white fluorescent light, photon flux of 80 μmol/m^2 s) and set up at different temperatures of 21 or 28°C.

The general phenotypic effects of *ICA* genes on growth-related traits at different temperatures were analyzed as described previously (Zhu et al., 2015). Vegetative growth was quantified by measuring the maximum rosette diameter (for plants in the *ica1-2* background) or the length of leaves at the fifth to sixth position (in *ica2-1* background) after flowering initiation. In the latter case, we estimated the leaf area and the lengths of petioles and blades using ImageJ 1.46 software (http://rsb.info.nih.gov/ij/). Flowering time was calculated as the number of days from seedling planting to opening of the first flower, and total leaf number was measured as the final number of rosette plus cauline leaves. Growth during the reproductive phase was estimated based on the length of the first 10 fruits in the main inflorescence, which is an indirect measurement of fertility and seed production (Alonso-Blanco et al., 1999). For phenotypic analyses, all transgenic lines and parental controls were grown simultaneously in the same experiment. A three complete blocks design with randomization was used, with each block containing one pot with six plants per line.

DNA Content and DNA Damage Measurements

DNA contents in cells were measured by flow cytometry using leaves of 14-d-old plants. Fresh tissue from a single plant grown at 21 or 28°C was chopped in Galbraith nuclear buffer (Galbraith et al., 1983) with a sharp razor. Nuclei were stained with propidium iodide and loaded into a cytometer (Cytomics FC500, Beckman Coulter) to obtain the distribution of DNA content in cell populations. The numbers of cells with high ploidy levels (C16, C32, and C64) were statistically compared among genotypes and transgenic lines using the average counts of three biological replicates (samples collected from different plants) in chi-square tests in contingency tables.

The first leaf assay was used to measure DNA damage sensitivity using the method of Rosa et al. (2013) as described in Zhu et al. (2015). In brief, 4-d-old seedlings grown in plates with 0.5× Murashige and Skoog (MS) solid medium were treated with a DNA damaging agent, the radiomimetic drug BLEO (Millipore; 1 μg/mL in 0.5× MS liquid medium), for 5 d. The BLEO-treated seedlings were thoroughly washed with 0.5× MS liquid medium and transferred to solid MS plates. The development of the first pair of leaves was scored 24 h later. Plants for this experiment were grown at 21°C in a growth chamber supplemented with light to provide a long-day photoperiod (16 h of cool-white fluorescent light, photon flux of 80 μmol/m^2 s).

ICA2 Sequences, Constructs, and Transgenic Lines

An *ICA2* genomic fragment of 5.6 kb was sequenced from Don-0 and L*er*, including 1.3 kb of promoter sequence and 5′ untranslated region; 3.5 kb of coding sequence; and 0.8 kb of the 3′ region. Both the 5′ and 3′ regions overlapped with neighboring genes. For sequencing, 10 overlapping 0.8- to 1.2-kb fragments were PCR amplified (Supplemental Table 3), and the products were sequenced using an ABI PRISM 3700 DNA analyzer. DNA sequences were aligned using DNASTAR 8.0 (Lasergene), and the alignments were inspected and edited by hand with GENEDOC (Nicholas et al., 1997).

The two 5.6-kb *ICA2* genomic fragments from Don-0 and L*er* were cloned in the pCAMBIA 3300 binary vector (CAMBIA) using standard molecular biology techniques. These fragments were PCR amplified using Phusion high-fidelity DNA polymerase (New England Biolabs), cloned in *Bam*HI cloning site, and checked by sequencing (Supplemental Table 3).

The *ICA2* genomic constructs were transferred by electroporation into *Agrobacterium tumefaciens* strain AGL0u (Lazo et al., 1991), and *ica1-2* or *ica2-1* Arabidopsis plants were transformed by the floral dip method (Clough and Bent, 1998). T_1 transformants were screened based on glufosinate resistance, and lines carrying single insertions were selected based on segregation of the resistance trait in T_2 family plants. Six to eight independent homozygous T_3 lines were selected for each construct and genetic background; their transgene and endogenous *ICA1* and *ICA2* alleles were verified by PCR prior to phenotypic analyses (Supplemental Table 3).

Phylogenetic Analysis

Intraspecific relationships among genomic and protein sequences from the 1001 Genomes Project (1001 Genomes Consortium, 2016) were determined by neighbor-joining analysis using MEGA7 (Tamura et al., 2011) and applying 10,000 bootstrap permutations to determine statistical significances. The haplotype network of ICA2 proteins was constructed using NETWORK 5 (http://www.fluxus-engineering.com) using the median-joining method.

Most *ICA/Thg1* sequences from different plant species were obtained from 54 whole-genome sequences that are fully assembled and annotated at Phytozome v12 (phytozome.jgi.doe.gov). Additional sequences from the genome projects of *Camelina sativa*, *Arabis alpina*, *Brassica napus*, and *Rapahanus sativus*, as well as nonplant model organisms, were obtained from GenBank (Supplemental Table 4). Physical distances between *ICA* genes of the same species were determined based on their physical positions in genome contigs. Microsynteny analyses were performed using Web-based SynMap software as implemented in the Comparative Genomics CoGe platform (genomevolution.org/coge; Lyons and Freeling, 2008; Haug-Baltzell et al., 2017). The alignment of proteins was obtained with CLUSTAL (https://www.ebi.ac.uk/Tools/msa/clustalo/) and edited by hand with GENEDOC (Nicholas et al., 1997; Supplemental File). The phylogenetic relationships among ICA proteins were determined by constructing an ML tree using MEGA7 (Tamura et al., 2011) and applying 10,000 bootstrap permutations for statistical significances.

Gene Expression Analysis

For expression analyses of *ICA* genes, plants were grown as described for phenotypic analyses but in pots containing ~50 plants, and plants from two blocks were mixed before RNA isolation. RNA from 14- to 18-d-old plants grown at different temperatures was isolated from whole rosette tissue using TRIzol reagent (Invitrogen) according to the manufacturer's protocol. Potential DNA contamination was removed by DNase digestion, and subsequent RNA purification was performed using a High Pure RNA isolation kit (Roche). cDNA was synthesized from 3 μg of total RNA using avian myeloblastosis virus reverse transcriptase (Invitrogen) and dT15 oligonucleotides. *ICA1* and *ICA2* expression was analyzed by quantitative RT-PCR using one and two pairs of oligonucleotides, respectively (Supplemental Table 3). To avoid amplification differences caused by DNA polymorphisms, primers were designed in gene regions differentiated between *ICA1* and *ICA2* but carrying no polymorphism among Col, L*er*, and Don-0. The ubiquitin-conjugating enzyme 21 gene (*At5g25760*), whose expression levels are highly steady among organs and environments (Czechowski et al., 2005), was used as an endogenous control for RNA sample standardization (Supplemental Table 3). All genes were amplified with Power SYBR Green Mix in a 7300 real-time PCR system (Applied Biosystems) and quantified using the standard curve method. Means and SES were derived from three biological replicates (RNA isolated from plants grown in different pots) for parental accessions or from three technical replicates (quantitative RT-PCR wells from the same cDNA sample) for transgenic lines.

Climatic and Statistical Analyses

To test the association between *ICA2* polymorphisms and climate, we extracted the 19 BIO climatic variables of the original accession locations from the world climate database (http://www.worldclim.org). General linear models were applied using climatic measurements as dependent variables and single-nucleotide polymorphisms as independent explanatory factors. To reduce the effect of genetic structure on climatic associations, the ancestry membership proportions of each accession in nine genetic groups (1001 Genomes Consortium, 2016) were included as covariates in general linear model analyses. Since the *ICA2*-L*er* haplogroup was mainly present in genetic groups 3, 5, and 6, tests were performed using all 687 accessions with the two major *ICA2* haplogroups, or only the 159 accessions from those three genetic groups.

The phenotypic effects of transgene, transgenic line, and temperature were tested statistically via mixed model analyses of variance, including transgene, temperature, and temperature × transgene interaction as the fixed effects and line (nested within transgenes) as the random effect factor (Supplemental Table 1). Tukey's honest significant difference test was used to compare the differences among the two types of transgenic lines grown at two different temperatures within the interaction term. These analyses were performed with the statistical packages SPSS 24 or Statistica 8.

Accession Numbers

Sequence data from this article can be found in the GenBank/EMBL libraries under the following accession numbers: MK056185 and MK056186.

Supplemental Data

Supplemental Figure 1. Analysis of the *ica2-1* insertional mutant.

Supplemental Figure 2. Search for the *ica1-2 ica2-1* double mutant.

Supplemental Figure 3. Differential complementation by natural alleles of *ICA2*.

Supplemental Figure 4. Flow cytometry analyses of nuclear DNA content at 21°C.

Supplemental Figure 5. Microsynteny relationships within *ICA1/ICA2* genomic regions in Camelineae species.

Supplemental Table 1. ANOVA tables.

Supplemental Table 2. Markers used for *ICA2* fine mapping.

Supplemental Table 3. Oligonucleotides used for *ICA2* analyses.

Supplemental Table 4. GenBank codes of ICA/Thg1 proteins.

Supplemental File. Alignment of ICA2 proteins from plants and model organisms.

ACKNOWLEDGMENTS

We thank Mercedes Ramiro for technical assistance. This work has been funded by the Agencia Estatal de Investigación of Spain and the Fondo Europeo de Desarrollo Regional (Unión Europea) (grant BIO2016-75754-P to C.A.-B.) and by the Australian Research Council (Discovery grant DP0983875 and ARC-Future Fellowship FT100100377 to S.B.).

AUTHOR CONTRIBUTIONS

C.A.-B., B.M.-V., I.A., and S.B. designed the study. B.M.-V., I.A., A.M.-M., and W.Z. performed the experiments. C.A.-B., B.M.-V., I.A., S.B., and W.Z. analyzed and interpreted the data. B.M.-V. and C.A.-B. wrote the article, with contributions from all other authors.

Received February 26, 2019; revised March 29, 2019; accepted April 12, 2019; published April 16, 2019.

REFERENCES

1001 Genomes Consortium (2016). 1,135 Genomes reveal the global pattern of polymorphism in *Arabidopsis thaliana*. Cell **166:** 481–491.

Alcázar, R., García, A.V., Kronholm, I., de Meaux, J., Koornneef, M., Parker, J.E., and Reymond, M. (2010). Natural variation at *Strubbelig Receptor Kinase 3* drives immune-triggered incompatibilities between *Arabidopsis thaliana* accessions. Nat. Genet. **42:** 1135–1139.

Alcázar, R., Pecinka, A., Aarts, M.G., Fransz, P.F., and Koornneef, M. (2012). Signals of speciation within *Arabidopsis thaliana* in comparison with its relatives. Curr. Opin. Plant Biol. **15:** 205–211.

Alings, F., Sarin, L.P., Fufezan, C., Drexler, H.C., and Leidel, S.A. (2015). An evolutionary approach uncovers a diverse response of tRNA 2-thiolation to elevated temperatures in yeast. RNA **21:** 202–212.

Alonso-Blanco, C., Blankestijn-de Vries, H., Hanhart, C.J., and Koornneef, M. (1999). Natural allelic variation at seed size loci in relation to other life history traits of *Arabidopsis thaliana.* Proc. Natl. Acad. Sci. USA **96:** 4710–4717.

Balasubramanian, S., Sureshkumar, S., Lempe, J., and Weigel, D. (2006). Potent induction of *Arabidopsis thaliana* flowering by elevated growth temperature. PLoS Genet. **2:** e106.

Bikard, D., Patel, D., Le Metté, C., Giorgi, V., Camilleri, C., Bennett, M.J., and Loudet, O. (2009). Divergent evolution of duplicate genes leads to genetic incompatibilities within *A. thaliana.* Science **323:** 623–626.

Bita, C.E., and Gerats, T. (2013). Plant tolerance to high temperature in a changing environment: Scientific fundamentals and production of heat stress-tolerant crops. Front. Plant Sci. **4:** 273.

Bomblies, K. (2010). Doomed lovers: Mechanisms of isolation and incompatibility in plants. Annu. Rev. Plant Biol. **61:** 109–124.

Bomblies, K., Lempe, J., Epple, P., Warthmann, N., Lanz, C., Dangl, J.L., and Weigel, D. (2007). Autoimmune response as a mechanism for a Dobzhansky-Muller-type incompatibility syndrome in plants. PLoS Biol. **5:** e236.

Box, M.S., et al. (2015). *ELF3* controls thermoresponsive growth in Arabidopsis. Curr. Biol. **25:** 194–199.

Brock, M.T., Maloof, J.N., and Weinig, C. (2010). Genes underlying quantitative variation in ecologically important traits: *PIF4* (phytochrome interacting factor 4) is associated with variation in internode length, flowering time, and fruit set in *Arabidopsis thaliana.* Mol. Ecol. **19:** 1187–1199.

Caicedo, A.L., Richards, C., Ehrenreich, I.M., and Purugganan, M.D. (2009). Complex rearrangements lead to novel chimeric gene fusion polymorphisms at the *Arabidopsis thaliana MAF2-5* flowering time gene cluster. Mol. Biol. Evol. **26:** 699–711.

Clough, S.J., and Bent, A.F. (1998). Floral dip: A simplified method for *Agrobacterium*-mediated transformation of *Arabidopsis thaliana.* Plant J. **16:** 735–743.

Czechowski, T., Stitt, M., Altmann, T., Udvardi, M.K., and Scheible, W.R. (2005). Genome-wide identification and testing of superior reference genes for transcript normalization in Arabidopsis. Plant Physiol. **139:** 5–17.

Edvardson, S., Elbaz-Alon, Y., Jalas, C., Matlock, A., Patel, K., Labbé, K., Shaag, A., Jackman, J.E., and Elpeleg, O. (2016). A mutation in the *THG1L* gene in a family with cerebellar ataxia and developmental delay. Neurogenetics **17:** 219–225.

Fernández, V., Takahashi, Y., Le Gourrierec, J., and Coupland, G. (2016). Photoperiodic and thermosensory pathways interact through *CONSTANS* to promote flowering at high temperature under short days. Plant J. **86:** 426–440.

Franks, S.J., Weber, J.J., and Aitken, S.N. (2014). Evolutionary and plastic responses to climate change in terrestrial plant populations. Evol. Appl. **7:** 123–139.

Galbraith, D.W., Harkins, K.R., Maddox, J.M., Ayres, N.M., Sharma, D.P., and Firoozabady, E. (1983). Rapid flow cytometric analysis of the cell cycle in intact plant tissues. Science **220:** 1049–1051.

Gallego-Bartolomé, J., Minguet, E.G., Marín, J.A., Prat, S., Blázquez, M.A., and Alabadí, D. (2010). Transcriptional diversification and functional conservation between DELLA proteins in Arabidopsis. Mol. Biol. Evol. **27:** 1247–1256.

Gu, W., Jackman, J.E., Lohan, A.J., Gray, M.W., and Phizicky, E.M. (2003). tRNAHis maturation: An essential yeast protein catalyzes addition of a guanine nucleotide to the 5′ end of tRNAHis. Genes Dev. **17:** 2889–2901.

Hanikenne, M., Talke, I.N., Haydon, M.J., Lanz, C., Nolte, A., Motte, P., Kroymann, J., Weigel, D., and Krämer, U. (2008). Evolution of metal hyperaccumulation required cis-regulatory changes and triplication of *HMA4.* Nature **453:** 391–395.

Haug-Baltzell, A., Stephens, S.A., Davey, S., Scheidegger, C.E., and Lyons, E. (2017). SynMap2 and SynMap3D: Web-based whole-genome synteny browsers. Bioinformatics **33:** 2197–2198.

Heinemann, I.U., Nakamura, A., O'Donoghue, P., Eiler, D., and Söll, D. (2012). tRNAHis-guanylyltransferase establishes tRNAHis identity. Nucleic Acids Res. **40:** 333–344.

Huang, C.H., et al. (2016). Resolution of Brassicaceae phylogeny using nuclear genes uncovers nested radiations and supports convergent morphological evolution. Mol. Biol. Evol. **33:** 394–412.

Jung, J.H., et al. (2016). Phytochromes function as thermosensors in Arabidopsis. Science **354:** 886–889.

Kliebenstein, D.J. (2008). A role for gene duplication and natural variation of gene expression in the evolution of metabolism. PLoS One **3:** e1838.

Kliebenstein, D.J., Lambrix, V.M., Reichelt, M., Gershenzon, J., and Mitchell-Olds, T. (2001). Gene duplication in the diversification of secondary metabolism: Tandem 2-oxoglutarate-dependent dioxygenases control glucosinolate biosynthesis in Arabidopsis. Plant Cell **13:** 681–693.

Kroymann, J., Donnerhacke, S., Schnabelrauch, D., and Mitchell-Olds, T. (2003). Evolutionary dynamics of an Arabidopsis insect resistance quantitative trait locus. Proc. Natl. Acad. Sci. USA **100** (Suppl 2): 14587–14592.

Kumar, S.V., Lucyshyn, D., Jaeger, K.E., Alós, E., Alvey, E., Harberd, N.P., and Wigge, P.A. (2012). Transcription factor PIF4 controls the thermosensory activation of flowering. Nature **484:** 242–245.

Lazo, G.R., Stein, P.A., and Ludwig, R.A. (1991). A DNA transformation-competent Arabidopsis genomic library in *Agrobacterium*. Biotechnology (N. Y.) **9:** 963–967.

Lee, J.H., Ryu, H.S., Chung, K.S., Posé, D., Kim, S., Schmid, M., and Ahn, J.H. (2013). Regulation of temperature-responsive flowering by MADS-box transcription factor repressors. Science **342:** 628–632.

Lee, K., Lee, E.H., Son, J., and Hwang, K.Y. (2017). Crystal structure of $tRNA^{His}$ guanylyltransferase from *Saccharomyces cerevisiae*. Biochem. Biophys. Res. Commun. **490:** 400–405.

Legris, M., Klose, C., Burgie, E.S., Rojas, C.C., Neme, M., Hiltbrunner, A., Wigge, P.A., Schäfer, E., Vierstra, R.D., and Casal, J.J. (2016). Phytochrome B integrates light and temperature signals in Arabidopsis. Science **354:** 897–900.

Lutz, U., Posé, D., Pfeifer, M., Gundlach, H., Hagmann, J., Wang, C., Weigel, D., Mayer, K.F., Schmid, M., and Schwechheimer, C. (2015). Modulation of ambient temperature-dependent flowering in *Arabidopsis thaliana* by natural variation of *FLOWERING LOCUS M.* PLoS Genet. **11:** e1005588.

Lutz, U., Nussbaumer, T., Spannagl, M., Diener, J., Mayer, K.F., and Schwechheimer, C. (2017). Natural haplotypes of *FLM* noncoding sequences fine-tune flowering time in ambient spring temperatures in Arabidopsis. eLife **6:** e22114.

Lynch, M. (2007). The Origins of Genomic Architecture. (Sunderland, MA: Sinauer Associates).

Lynch, M., and Katju, V. (2004). The altered evolutionary trajectories of gene duplicates. Trends Genet. **20:** 544–549.

Lyons, E., and Freeling, M. (2008). How to usefully compare homologous plant genes and chromosomes as DNA sequences. Plant J. **53:** 661–673.

McClung, C.R., Lou, P., Hermand, V., and Kim, J.A. (2016). The importance of ambient temperature to growth and the induction of flowering. Front. Plant Sci. **7:** 1266.

Méndez-Vigo, B., Savic, M., Ausín, I., Ramiro, M., Martín, B., Picó, F.X., and Alonso-Blanco, C. (2016). Environmental and genetic interactions reveal *FLOWERING LOCUS C* as a modulator of the natural variation for the plasticity of flowering in Arabidopsis. Plant Cell Environ. **39:** 282–294.

Nicholas, K.B., Nicholas, H.B.J., and Deerfield, D.W. (1997). GeneDoc: Analysis and visualization of genetic variation. Embnet.news **4:** 1–4.

Nicotra, A.B., Atkin, O.K., Bonser, S.P., Davidson, A.M., Finnegan, E.J., Mathesius, U., Poot, P., Purugganan, M.D., Richards, C.L., Valladares, F., and van Kleunen, M. (2010). Plant phenotypic plasticity in a changing climate. Trends Plant Sci. **15:** 684–692.

Orioli, A. (2017). tRNA biology in the omics era: Stress signalling dynamics and cancer progression. BioEssays **39:** 3.

Panchy, N., Lehti-Shiu, M., and Shiu, S.H. (2016). Evolution of gene duplication in plants. Plant Physiol. **171:** 2294–2316.

Phillips, P.C. (2008). Epistasis--The essential role of gene interactions in the structure and evolution of genetic systems. Nat. Rev. Genet. **9:** 855–867.

Placido, A., Sieber, F., Gobert, A., Gallerani, R., Giegé, P., and Maréchal-Drouard, L. (2010). Plant mitochondria use two pathways for the biogenesis of tRNAHis. Nucleic Acids Res. **38:** 7711–7717.

Prasad, K.V., et al. (2012). A gain-of-function polymorphism controlling complex traits and fitness in nature. Science **337:** 1081–1084.

Quint, M., Delker, C., Franklin, K.A., Wigge, P.A., Halliday, K.J., and van Zanten, M. (2016). Molecular and genetic control of plant thermomorphogenesis. Nat. Plants **2:** 15190.

Raina, M., and Ibba, M. (2014). tRNAs as regulators of biological processes. Front. Genet. **5:** 171.

Raschke, A., et al. (2015). Natural variants of *ELF3* affect thermomorphogenesis by transcriptionally modulating PIF4-dependent auxin response genes. BMC Plant Biol. **15:** 197.

Rice, T.S., Ding, M., Pederson, D.S., and Heintz, N.H. (2005). The highly conserved tRNAHis guanylyltransferase *Thg1p* interacts with the origin recognition complex and is required for the G2/M phase transition in the yeast *Saccharomyces cerevisiae.* Eukaryot. Cell **4:** 832–835.

Rosa, M., Von Harder, M., Cigliano, R.A., Schlögelhofer, P., and Mittelsten Scheid, O. (2013). The Arabidopsis SWR1 chromatin-remodeling complex is important for DNA repair, somatic recombination, and meiosis. Plant Cell **25:** 1990–2001.

Sanchez-Bermejo, E., and Balasubramanian, S. (2016). Natural variation involving deletion alleles of *FRIGIDA* modulate temperature-sensitive flowering responses in *Arabidopsis thaliana.* Plant Cell Environ. **39:** 1353–1365.

Soltis, P.S., and Soltis, D.E. (2016). Ancient WGD events as drivers of key innovations in angiosperms. Curr. Opin. Plant Biol. **30:** 159–165.

Sureshkumar, S., Dent, C., Seleznev, A., Tasset, C., and Balasubramanian, S. (2016). Nonsense-mediated mRNA decay modulates *FLM*-dependent thermosensory flowering response in Arabidopsis. Nat. Plants **2:** 16055.

Tamura, K., Peterson, D., Peterson, N., Stecher, G., Nei, M., and Kumar, S. (2011). MEGA5: Molecular evolutionary genetics analysis using maximum likelihood, evolutionary distance, and maximum parsimony methods. Mol. Biol. Evol. **28:** 2731–2739.

Tasset, C., Singh Yadav, A., Sureshkumar, S., Singh, R., van der Woude, L., Nekrasov, M., Tremethick, D., van Zanten, M., and Balasubramanian, S. (2018). *POWERDRESS*-mediated histone deacetylation is essential for thermomorphogenesis in *Arabidopsis thaliana.* PLoS Genet. **14:** e1007280.

Trontin, C., Kiani, S., Corwin, J.A., Hématy, K., Yansouni, J., Kliebenstein, D.J., and Loudet, O. (2014). A pair of receptor-like kinases is responsible for natural variation in shoot growth response to mannitol treatment in *Arabidopsis thaliana.* Plant J. **78:** 121–133.

Vargas, P., and Zardoya, R. (2014). The Tree of Life. (Sunderland, MA: Sinauer Associates).

Verhage, L., Angenent, G.C., and Immink, R.G. (2014). Research on floral timing by ambient temperature comes into blossom. Trends Plant Sci. **19:** 583–591.

Vlad, D., et al. (2014). Leaf shape evolution through duplication, regulatory diversification, and loss of a homeobox gene. Science **343:** 780–783.

Vlad, D., Rappaport, F., Simon, M., and Loudet, O. (2010). Gene transposition causing natural variation for growth in *Arabidopsis thaliana.* PLoS Genet. **6:** e1000945.

Zhu, L., Ow, D.W., and Dong, Z. (2018). Transfer RNA-derived small RNAs in plants. Sci. China Life Sci. **61:** 155–161.

Zhu, W., Ausin, I., Seleznev, A., Méndez-Vigo, B., Picó, F.X., Sureshkumar, S., Sundaramoorthi, V., Bulach, D., Powell, D., Seemann, T., Alonso-Blanco, C., and Balasubramanian, S. (2015). Natural variation identifies *ICARUS1*, a universal gene required for cell proliferation and growth at high temperatures in *Arabidopsis thaliana.* PLoS Genet. **11:** e1005085.